phys. stat. sol. (a) **164**, 567 (1997)

Subject classification: 71.35.Ji; 78.20.Ls; 78.66.Fd; S7.12

Terahertz Linear and Nonlinear Dynamics in Confined Magnetoexcitons

J. KONO[1]) (a, b), M.Y. SU (b), K.B. NORDSTROM (b), J. ČERNE[2]) (b), M.S. SHERWIN (b), S.J. ALLEN, JR. (b), T. INOSHITA (a), T. NODA (c), H. SAKAKI (a, c), G.E.W. BAUER (d), M. SUNDARAM[3]) (e), and A.C. GOSSARD (e)

(a) Quantum Transition Project, Japan Science and Technology Corporation, Tokyo 153, Japan.

(b) Center for Terahertz Science and Technology and Department of Physics, University of California, Santa Barbara, California 93106, USA

(c) Institute of Industrial Science, University of Tokyo, Tokyo 106, Japan

(d) Department of Applied Physics, Delft University of Technology, 2628 CJ Delft, The Netherlands

(e) Materials Department, University of California, Santa Barbara, California 93106, USA

(Received September 1, 1997)

We have probed the linear and nonlinear terahertz (THz) properties of magnetoexcitons in GaAs/AlGaAs quantum wells. By monitoring photoluminescence from the quantum wells that were simultaneously driven by THz fields, we have directly observed *internal transitions* of excitons. In the nonlinear, high-THz-excitation regime, we observed mixing of optical and THz radiation, which resulted in THz *optical sidebands*. By monitoring the sidebands, we observed one- and two-THz-photon nonlinear internal transitions in excitons. These results provide new and accurate information on the energy structure and internal dynamics of excitons.

Introduction. The fundamental importance and much of the rich structure of excitons have been revealed by extensive studies using interband optical spectroscopy (≈1.5 eV in GaAs) for the past several decades. However, very limited research has succeeded in directly exploring the *internal* dynamics of excitons [1,2]. In such studies near-infrared (NIR) photons create excitons, and then far-IR/THz radiation (of order 10 meV, 2.5 THz, or 100 μm) manipulates them. The short lifetimes (≈0.5 ns) of direct quantum-well (QW) excitons make it extremely difficult to achieve the large population of cold excitons required for THz absorption studies. Using a new type of optical detection technique, we have carried out linear and nonlinear THz spectroscopies, both of which provide new

---

[1]) Present address: Stanford Picosecond FEL Center, W.W. Hansen Experimental Physics Laboratory, Stanford University, Stanford, CA 94305-4085, USA.

[2]) Present address: Department of Physics, Condensed Matter Physics, University of Maryland at College Park, College Park, MD 20742, USA.

[3]) Present address: JPL, NASA, NS 302-231, 4800 Oak Grove Drive, Pasadena, CA 91109, USA.

insight into the internal structure and dynamics of confined magnetoexcitons in GaAs/AlGaAs QWs.

Sample and Experimental Methods. The sample consisted of 25 periods of undoped GaAs/$Al_{0.3}Ga_{0.7}As$ (10 nm/15 nm) multiple QWs. The UCSB Free-Electron Lasers (FELs) provided intense THz radiation (up to 20 kW) that can be continuously tuned from 0.12 to 4.75 THz (4 to 160 cm^{-1}). In the linear THz spectroscopy, an Ar^+ laser or a tunable cw Ti:sapphire laser was used to create electron–hole pairs in the QWs. The resulting photoluminescence (PL) was detected by a photomultiplier tube. The change in PL induced by THz radiation was recorded as a function of magnetic field, B. For sideband generation, we used a geometry in which NIR radiation from the Ti:sapphire laser passed through the sample collinearly with strong THz radiation from the FELs. The produced sidebands were detected by a CCD-camera.

Experimental Results. Figure 1 shows a typical linear THz spectrum obtained for the GaAs QWs. Here the intensity of the heavy-hole (HH) exciton PL in the presence of THz radiation with a frequency of 103 cm^{-1} is plotted as a function of B. The PL intensity is normalized to the intensity in the absence of THz radiation at all B. It can be seen that whenever the THz radiation is absorbed resonantly by the system, the PL intensity decreases resonantly. Three THz resonances are clearly observed. As discussed in the fourth section, we assign these resonances to 1s → $3p_-$ ((00) → (12)), 1s → $2p_+$ ((00) → (10)), and $2p_-$ → 2s ((01) → (11)) excitonic transitions in the low-field hydrogenic (high-field Landau) notation, represented by the dotted, dashed, and solid arrows, respectively, in the figure.

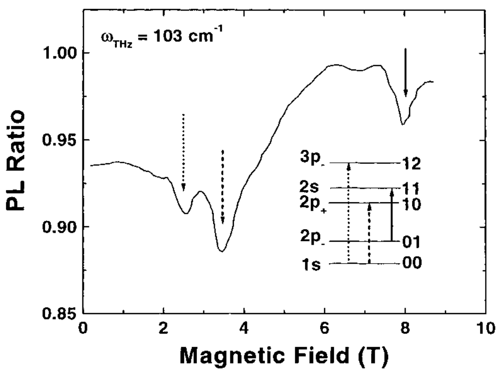

Fig. 1

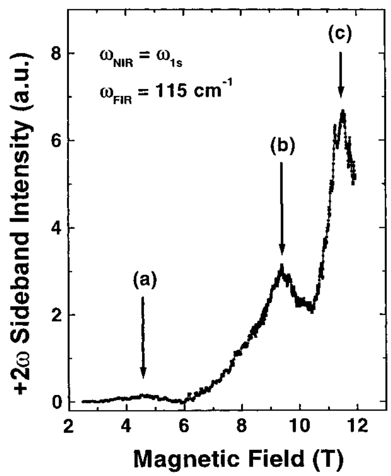

Fig. 2

Fig. 1. Internal transitions of excitons observed for undoped 10 nm GaAs QWs. The ratio of the PL amplitude with and without THz irradiation is plotted as a function of magnetic field at a THz frequency of 103 cm^{-1}

Fig. 2. *Nonlinear* internal transitions of excitons. The intensity of the $+2\omega$ sideband intensity is plotted against B. ω_{THz} = 115 cm^{-1} and $\omega_{NIR} = \omega_{1s}$ at all B. Pronounced resonances occur when (a) $\omega_{THz} = \omega_{2p+} - \omega_{1s}$, (b) $2\omega_{THz} = \omega_{2s} - \omega_{1s}$, and (c) $\omega_{THz} = \omega_{2p-} - \omega_{1s}$

Fig. 2 shows a typical *nonlinear* THz spectrum. Here the intensity of the generated $+2\omega$ sideband [3] is plotted as a function of B for $\omega_{\mathrm{THz}} = 115\ \mathrm{cm}^{-1}$ with $\omega_{\mathrm{NIR}} = \omega_{1\mathrm{s}}$ at all magnetic fields, where $\omega_{1\mathrm{s}}$ is the creation frequency for 1s HH excitons. There are three distinct resonances at 4.5, 9.5, and 11.5 T, labeled as (a), (b), and (c), respectively. These resonances occur when (a) $\omega_{\mathrm{THz}} = \omega_{2\mathrm{p}+} - \omega_{1\mathrm{s}}$, (b) $2\omega_{\mathrm{THz}} = \omega_{2\mathrm{s}} - \omega_{1\mathrm{s}}$, and (c) $\omega_{\mathrm{THz}} = \omega_{2\mathrm{p}-} - \omega_{1\mathrm{s}}$, in the low-field hydrogenic notation. The resonance positions are in excellent agreement with those expected from the linear ODTR spectroscopy [1] and theory [4].

Discussion. In general, many quantum numbers are necessary to specify a state of QW excitons: subband indices $(i,\ j)$, the principal quantum number n, the angular momentum projection m_z, the center-of-mass momentum $\mathbf{K}$, the electron spin M, and the hole spin M'. Here we concentrate on the in-plane motion of the immobile ($\mathbf{K} = 0$) excitons in the lowest subbands ($i = j = 1$, $(M,\ M') = (\pm 1/2,\ \pm 3/2)$) since these are the relevant optically-active exciton states. Hence we can simply use the 2D hydrogenic quantum numbers $(n,\ m_z)$ to refer to an exciton state, e.g., the 1 s state is $|n = 1;\ m_z = 0\rangle$. In high B, where the system consists of "Coulomb-shifted" Landau levels, more convenient notation is the Landau-level notation $(N,\ M)$, where N (M) represents the electron (hole) Landau index. The low-field–high-field correspondence is given by the simple relations, $n = \max\,(N,\ M) + 1$ and $m_z = N - M$, e.g., 1s $\leftrightarrow$ $(N,\ M) = (00)$, $2\mathrm{p}_+ \leftrightarrow (10)$, etc. [5]. The selection rule for exciton internal transitions is $\Delta m_z = \pm 1$ for $\sigma^{\pm}$ circular polarizations. For σ^+ polarization, e.g., 1s $\rightarrow$ $2\mathrm{p}_+$ ((00) $\rightarrow$ (10)), 1s $\rightarrow$ $3\mathrm{p}_+$ ((00) $\rightarrow$ (21)), in the low-field (high-field) notation, are expected.

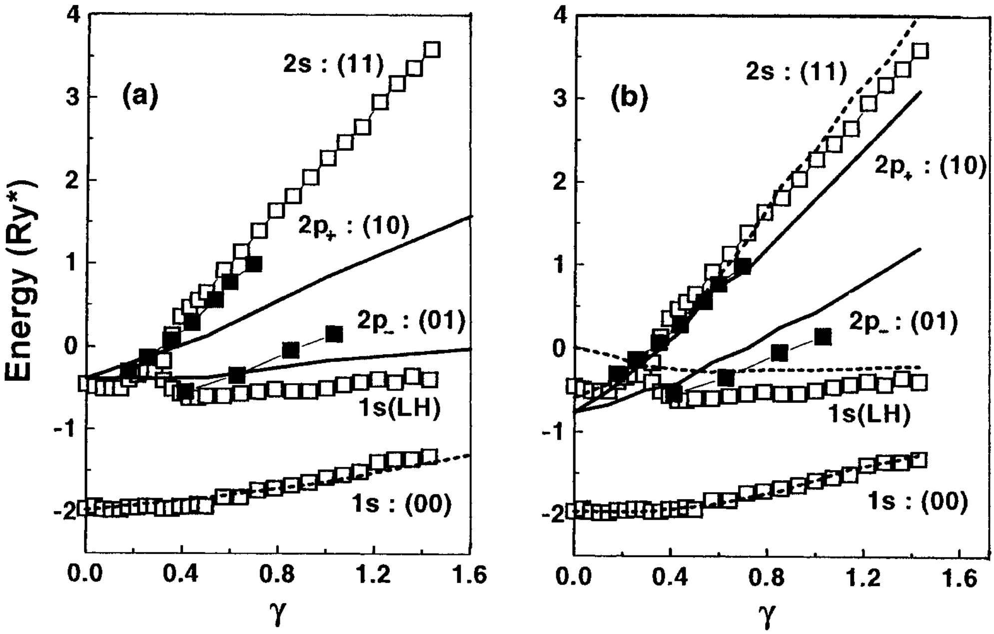

Fig. 3. Low-lying energy levels vs. dimensionless magnetic field $\gamma = \hbar\omega_c/2R^*$ for excitons in 10 nm-wide GaAs quantum wells. Solid squares (s-states): data from interband absorption, open squares (p-states): data from linear and nonlinear THz spectroscopies, dashed lines: theory for s-states, and solid lines: theory for p-states. Theory: a) [6] and b) [4]

In Fig. 3 the four low-lying HH exciton levels (1s, $2p_\pm$, 2s) and the 1s LH exciton level, deduced from interband (s-states) and intraband (p-states) transitions, are compared with two different theories. The first theory, due to Greene and Bajaj [6], is a hydrogenic, reduced-mass theory. Here the reduced mass of the electrons and holes is the only adjustable parameter. By setting this parameter to an unrealistically large value ($\approx 0.1 m_0$, where m_0 is the mass of an electron in vacuum), we can approximately fit the 1s HH state. However, with the same mass, the slopes versus B for the $2p_+$ and $2p_-$ HH states are too small to fit the data, as can be seen in Fig. 3a. The theoretical curves in Fig. 3b were obtained from a paper by Bauer and Ando [4], who calculated the energy levels of magnetoexcitons in 10 nm-wide GaAs QWs within the framework of the effective mass approximation, taking into account the valence-band complexities with a standard set of band parameters. We directly compared the experiment and theory with no adjustment. The obtained excellent agreement shown in Fig. 3b clearly shows the correctness of the experiment and theory, providing accurate information on these energy levels.

Acknowledgements. This work was supported by JST Quantum Transition Project, ONR N00014-K-0692, and QUEST DMR91-20007. The authors are grateful to T. Ando, A.B. Dzyubenko, A. Imamoglu, K. Johnsen for useful comments and discussions, and D.P. Enyeart, D.T. White and J.R. Allen at the Center for Terahertz Science and Technology for technical support.

References

[1] J. Černe, J. Kono, M.S. Sherwin, M. Sundaram, A.C. Gossard, and G.E.W. Bauer, Phys. Rev. Lett. **77**, 1131 (1996).
[2] M.S. Salib, H.A. Nickel, G.S. Herold, A. Petrou, B.D. McCombe, R. Chen, K.K. Bajaj, and W. Schaff, Phys. Rev. Lett. **77**, 1135 (1996).
[3] For THz optical sideband generation, see: J. Kono et al., in: The Physics of Semiconductors, Ed. M. Scheffler and R. Zimmermann, World Scientific Publ. Co., Singapore 1996 (p. 1911).
J. Černe et al., Appl. Phys. Lett. **70**, 3543 (1997).
J. Kono et al., Phys. Rev. Lett. **79**, 1758 (1997).
[4] G.E.W. Bauer and T. Ando, Phys. Rev. B **38**, 6015 (1988).
[5] A.H. MacDonald and D.S. Ritchie, Phys. Rev. B **33**, 8336 (1986).
[6] R.L. Greene and K.K. Bajaj, Phys. Rev. B **31**, 913 (1985).